On the Assessment of the Flexibility Region in Inter-DSO Local Markets

Ángel Paredes , José A. Aguado
Department of Electrical Engineering
University of Málaga
Málaga, Spain
angelparedes@uma.es, jaguado@uma.es
*

July 3, 2023

Abstract

Renewable Distributed Energy Resources (RDERs) are being rapidly deployed in energy systems to meet net zero emissions objectives. RDERs may cause operational issues in these systems, which exposes both Transmission System Operators (TSOs) and Distribution System Operators (DSOs) to congestions and imbalances. Recently, efforts were made towards the definition of Inter-DSO Local Flexibility Markets (LFMs) to mitigate those issues. However, DSOs do not have properly tools that analyse their flexibility when participating in these markets. This paper presents a linear approach for assessing their flexibility region and the associated costs. The novelty of the proposed approach lies in the flexibility assessment in Inter-DSO LFMs and in the linearization of the problem, which enables the analysis of non-linear DERs such as batteries. The feasibility of the proposed approach is demonstrated using a case study based two IEEE 34 bus systems which represent two different DSOs participating in an Inter-DSO LFM. The flexibility of each DSO is analysed in two scenarios, when the interconnection is active and when it is congested. Results reflect how RDERs can effectively procure flexibility for both situations and how the proposed approach captures their non-linear behaviour.

Nomenclature

Parameters are in upper case letter and variables in lower case letter. $|\Omega|$ denotes the cardinality of the set Ω. The rest of the nomenclature is introduced in the text.

*Á. Paredes and J. A. Aguado work were partially supported by Junta de Andalucia (Spain) Project Ref: P20_01164, by Ministerio de Ciencia e Innovación through project TED2021-132339B-C42 and by the University of Málaga. Á. Paredes was also supported by the FPU grant (FPU19/03791) funded by the Spanish Ministry of Education. The authors thankfully acknowledge the computer resources provided by the SCBI center of the University of Málaga.

Indices and sets

a, Ω_a Index and set for flexible agents (Flexible Loads (FLs), Flexible Generators (FGs) and BESSs) $a \in \Omega_a$.
t, Ω_t Index and set for time periods, $t \in \Omega_t$.
i, j, Ω_i Indexes and set for buses, $(i, j) \in \Omega_i$.
n, Ω_n Index and set for DSOs of the market $n \in \Omega_n$.
h, Ω_h Index and set for McCormick Envelopes $h \in \Omega_h$.
k Index for discretization of feasible region.

Parameters

$\underline{B}_{i,j}, G_{i,j}$ Susceptance and conductance of the line i, j (S).
$\overline{S}_{i,j}$ Thermal limit of the line i, j (kVA).
$\pi_{a,t}, \rho_{a,t}$ Active and reactive flexibility bids of agent a in period t (€/kW, €/kVA).
$P^{sch}_{a,t}, Q^{sch}_{a,t}$ Scheduled sch active and reactive power for agent a in period t (kW, kVAr).
$\overline{SOC}_s, \underline{SOC}_s, SOC0_s$ Upper bound, lower bound and initial SOC of BESS s (kWh).

Variables

$\Delta p^n_{a,t}, \Delta q^n_{a,t}$ Active and reactive flexibility products of agent a in period t in upward (≥ 0) and downward (≤ 0) directions (kW, kVA).
$F^n_{p,t}, F^n_{q,t}$ Total quantity of active p and reactive q flexibility traded by DSO n in time period t (kW, kVAr).

1 Introduction

In a paradigm with high requirements for Renewable Distributed Energy Resources (RDERs) to meet net zero emissions objectives, operational contingencies may appear due to their nondeterministic nature [1]. In this scenario, flexibility is needed both at transmission and distribution level to solve these issues. Trading of flexibility products between Transmission System Operator (TSO) and Distribution System Operators (DSOs) is fundamental in this sense. However, contingencies can also appear in the interface between them, preventing the TSO from supporting the DSOs and vice-versa [2]. In this context, Inter-DSO Local Flexibility Markets (LFMs) offer a framework to relieve operational congestions, imbalances and voltage deviations without involving upstream assets [3]. This motivates to investigate how the flexibility region of RDERs connected to the distribution network can be estimated inside a Inter-DSO LFM paradigm.

When assessing the flexibility region of distribution systems, various search methodologies have been proposed. Monte-Carlo simulation is used in [4] and in [5] for the flexibility and feasibility assessment of virtual power plants and TSO/DSO interfaces. This method evaluates an extensive point cloud, which is randomly generated, obtaining the flexibility region as the convex hull of the feasible points. The outcome of this method highly depends on the type of sampling and in the initial selection of points [6], being necessary complex

methods to evaluate the feasible and flexible regions with precision. Besides, this methodology can be computational extensive, needing million of points to obtain a reliable solution. Another branch of research directly search for the boundary of the flexibility region, using a set of optimization problems. A linear search is used in [7] and in [8], this search algorithm first determines the overall limits of the region in the active and reactive dimensions, and then obtains intermediate points by discretizing the search space. A rotational angle method is used in [9]. In this method, a reference point inside the flexible region is used to compute the limits of the region by changing the search direction a determined angular quantity. This method assume that the flexibility region is convex and requires a reference point inside the feasible region. An interactive algorithm is proposed in [10] that is sequentially obtaining points in the boundary until the difference of the output area is less than a threshold, discarding those infeasible or non-optimal points obtained during the process. Another branch of research defines a multi-objective optimization for the active and reactive maximisation of the flexibility procurement, and solve it using epsilon-constrained method for AC network modelling [11] and LinDistFlow relaxation [12]. Moreover, a method based on Minkowsky addition is proposed in [13], which defines the flexible region as the Minkowsky sum of all the RDERs connected to the distribution network, however, being non-linear, this method can be computational expensive, and its optimal solution cannot be granted.

In terms of the types of RDERs included in the modelling, [7] evaluates the flexibility region at the TSO/DSO interface using a MINLP optimization problem for FLs and FGs. Similarly, authors in [9] propose a non-linear methodology to evaluate the flexibility region at the interconnection with the upstream network for controllable loads and fuel-based generation. Linearizing the problem, authors in [14] ensures finding the optimal solution of the problem, and thus the real flexibility region. They use Monte-Carlo simulation for a distribution network with FGs and FLs. However not considering the impact that distributed Battery Energy Storage Systems (BESSs) have in the flexibility, the outcome of the algorithm may underestimate the real capabilities of the grid. Authors in [15] evaluate the flexibility of virtual power plants considering the temporal constraints using a linear robust model which includes the uncertainty, but nor the network neither BESSs are integrated in the model. Besides of that, there is a gap in the knowledge when analysing the flexibility region at the DSO/DSO interface, i.e. when they participate in Inter-DSO LFMs.

This paper presents a linear approach to determine the flexibility region of the DSO participating in Inter-DSO LFMs. Costs maps associated to this flexibility procurement are also evaluated. The methodology uses McCormick envelopes and a polygonal inner approximation to linearize the problem and include BESS into the flexibility assessment. The major contributions of this paper are:

- A linear approach to assess the flexibility region of RDER in Inter-DSO LFMs. Non-linear restrictions are effectively linearized using a variable change, McCormick envelopes and a polygonal inner approximation of quadratic constraints.
- A methodology that can analyse the flexibility of distribution network even if the interconnection with the upstream network is congested or, by extension, there are multiple interconnections with upstream networks.

- An analysis of the influence of the TSO in the flexibility procurement of multiple DSOs and its associated cost maps.

The remainder of this paper is organised as follows. Section II formulates the optimization problem to estimate the flexibility region and linearize it. Section III presents simulation results considering the influence of the TSO. Lastly, Section IV concludes the paper.

2 Flexibility Estimation

In this section, the constraints and the objectives functions needed to determine the flexibility region of RDERs in Inter-DSO LFM are explained.

2.1 Agents

Flexible demands will modify their after-market schedule $p^{am}_{f,t}$ between an upper $\overline{P}_{f,t}$ and lower $\underline{P}_{f,t}$ limit, providing flexibility products $\Delta p_{f,t}$. It is assumed that the FLs cannot modify their reactive power consumption $Q^{sch}_{f,t}$. Thus,

$$p^{am}_{f,t} = P^{sch}_{f,t} + \Delta p_{f,t} \qquad \forall f \in \Omega_f, \forall t \in \Omega_t \quad (1a)$$

$$\underline{P}_{f,t} \leq p^{am}_{f,t} \leq \overline{P}_{f,t} \qquad \forall f \in \Omega_f, \forall t \in \Omega_t \quad (1b)$$

Similarly, FGs modify its schedule $p^{am}_{g,t}$ between a lower $\underline{P}_{g,t}$ and upper $\overline{P}_{g,t}$, offering $\Delta p_{g,t}$ flexibility in the LFM. Being renewable generators, $\overline{P}_{g,t}$ is equal to $P^{sch}_{g,t}$, then downward active flexibility is the only product FGs can offer. On the other hand, it is assumed that the PV solar inverter can control the production of reactive power $q^{am}_{g,t}$ [16]. Then, considering the inverter power rating S^{inv}_{g}

$$p^{am}_{g,t} = P^{sch}_{g,t} + \Delta p_{g,t} \qquad \forall g \in \Omega_g, \forall t \in \Omega_t \quad (2a)$$

$$0 \leq p^{am}_{g,t} \leq P^{sch}_{g,t} \qquad \forall g \in \Omega_g, \forall t \in \Omega_t \quad (2b)$$

$$q^{am}_{g,t} = Q^{sch}_{g,t} + \Delta q_{g,t} \qquad \forall g \in \Omega_g, \forall t \in \Omega_t \quad (2c)$$

$$p^{am2}_{g,t} + q^{am2}_{g,t} \leq {S^{inv}_{g}}^2 \qquad \forall g \in \Omega_g, \forall t \in \Omega_t \quad (2d)$$

BESSs provide both upward $p^{u}_{s,t}$ and downward $p^{d}_{s,t}$ flexibility. It is assumed that the State of Charge (SOC) of the BESS s is the same at the beginning and at the end of the day $soc_{s,0} = soc_{s,\|\Omega_t\|} = SOC0_s$. Converter can produce reactive power flexibility $\Delta q_{s,t}$. Let $\eta^{ch}_{s}, \eta^{dis}_{s}$ be the charging and discharging efficiencies, S^{conv}_{s} be the power rating of the converter and, $\underline{SOC}_s, \overline{SOC}_s$ be the lower and upper bound of the SOC of the BESS s, then

$$\left(p^{u}_{s,t} - p^{d}_{s,t}\right)^2 + {\Delta q_{s,t}}^2 \leq {S^{conv}_{s}}^2 \qquad \forall s \in \Omega_s, \forall t \in \Omega_t \quad (3a)$$

$$p^{u}_{s,t} \cdot p^{d}_{s,t} = 0 \qquad \forall s \in \Omega_s, \forall t \in \Omega_t \quad (3b)$$

$$soc_{s,t} = soc_{s,t-1} + \eta^{ch}_{s} p^{ch}_{s,t} - \frac{p^{d}_{s,t}}{\eta^{dis}_{s}} \qquad \forall s \in \Omega_s, \forall t \in \Omega_t \quad (3c)$$

$$\underline{SOC}_s \leq soc_{s,t} \leq \overline{SOC}_s \qquad \forall s \in \Omega_s, \forall t \in \Omega_t \quad (3d)$$

Equation (3b) is declared to avoid simultaneous activation of upward and downward flexibility directions.

2.2 Network model

We use a state-independent linear description of the power flows of the grid as in [17]. Let $v_{i,j,t}$ and $\theta_{i,j,t}$ be the voltage magnitude and phase angle difference between buses i and j, respectively. Active and reactive node balances are described by (4a) and (4b), while power flows are computed by (4c) and (4d), thermal limit is enforced by (4f).

$$\sum_{j\in\Omega_i}(G_{i,j}v_{j,t} - B_{i,j}\theta_{j,t}) = p_{i,t} \qquad \forall i\in\Omega_i, \forall t\in\Omega_t \quad (4a)$$

$$-\sum_{j\in\Omega_i}(B_{i,j}v_{j,t} + G_{i,j}\theta_{j,t}) = q_{i,t} \qquad \forall i\in\Omega_i, \forall t\in\Omega_t \quad (4b)$$

$$p_{i,j,t} = G_{i,j}v_{i,j,t} - B_{i,j}\theta_{i,j,t} \qquad \forall (i,j)\in\Omega_b, \forall t\in\Omega_t \quad (4c)$$

$$q_{i,j,t} = -B_{i,j}v_{i,j,t} - G_{i,j}\theta_{i,j,t} \qquad \forall (i,j)\in\Omega_b, \forall t\in\Omega_t \quad (4d)$$

$$p_{i,j,t}^2 + q_{i,j,t}^2 \leq \overline{S}_{i,j}^2 \qquad \forall (i,j)\in\Omega_b, \forall t\in\Omega_t \quad (4e)$$

$$-\pi \leq \theta_{i,t} \leq \pi, \;\; -\underline{V}_i \leq \theta_{i,t} \leq \overline{V}_i \qquad \forall i\in\Omega_i, \forall t\in\Omega_t \quad (4f)$$

2.3 Inter-DSO LFMs

Inter-DSO LFMs are marketplaces where flexibility is traded with the aim of solving operational problems such as, congestions, imbalances or voltage deviations. In this type of markets, the bids of the flexible assets are minimized to obtain the optimal schedule at minimum cost. However, because of the TSO not being involved in the operation, upstream power flow cannot be modified, i.e., upward and downward flexibility must be matched. Let $\pi_{a,t}$ and $\rho_{a,t}$ be the bid of the agent a in the time period t for active and reactive flexibility, respectively. Then, costs for assets a connected to DSO n are defined by

$$c_{a,t}^n = \pi_{a,t}^n \Delta p_{a,t}^n + \rho_{a,t}^n \Delta q_{a,t}^n \qquad \forall a\in\Omega_a, \forall t\in\Omega_t \quad (5a)$$

Upward and downward flexibility must be matched as the flexibility exchange is among n DSOs.

$$\sum_{n\in\Omega_n}\sum_{a\in\Omega_a^n}\Delta p_{a,t}^n = 0, \sum_{n\in\Omega_n}\sum_{a\in\Omega_a^n}\Delta q_{a,t}^n = 0 \qquad \forall t\in\Omega_t \quad (5b)$$

2.4 Linearization of the problem

In this section, the previously described restrictions are linearized. Equation (3b) is linearized using a variable change and McCormick envelopes [18], while (2d), (3a) and (4e) are linearized via a polygonal inner approximation [19]. Nonlinear restriction (3b) is linearized as follows. Let $y_{s,t}$ and $z_{s,t}$ be the auxiliary variables, they are defined as

$$y_{s,t} = (p_{s,t}^u + p_{s,t}^d)/2 \qquad \forall s\in\Omega_s, \forall t\in\Omega_t \quad (6a)$$

$$z_{s,t} = (p_{s,t}^u - p_{s,t}^d)/2 \qquad \forall s\in\Omega_s, \forall t\in\Omega_t \quad (6b)$$

Then, equation (3b) can be re-written as follows

$$y_{s,t}^2 - z_{s,t}^2 = 0 \qquad \forall s\in\Omega_s, \forall t\in\Omega_t \quad (6c)$$

Equation (6c) is linearized by replacing $y_{s,t}^2$ and $z_{s,t}^2$ by a set of linear inequalities defined by $u_{s,t}$ and $r_{s,t}$, respectively,

$$u_{s,t} - r_{s,t} = 0 \qquad \forall s \in \Omega_s, \forall t \in \Omega_t \quad (6d)$$

$$u_{s,t} \geq a_{h,s,t} \cdot z_{s,t} + b_{n,s,t} \qquad \forall h \in \Omega_h, \forall s \in \Omega_s, \forall t \in \Omega_t \quad (6e)$$

$$r_{s,t} \geq c_{h,s,t} \cdot z_{s,t} + d_{n,s,t} \qquad \forall h \in \Omega_h, \forall s \in \Omega_s, \forall t \in \Omega_t \quad (6f)$$

where $a_{h,s,t}$ and $b_{h,s,t}$ are the slopes of the linear inequalities while $c_{h,s,t}$ and $d_{h,s,t}$ are the independent terms of the equations. A pictorial representation of the feasible region defined by (6e) and (6f) is showed in Fig. 1 (a).

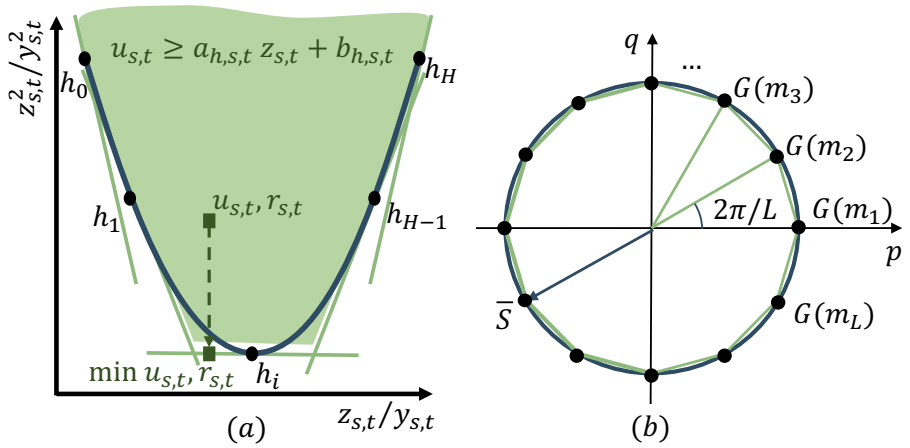

Figure 1: Pictorial example of the McCormick envelopes (a) and polygonal inner approximation of quadratic constraints (b).

Besides, the variables $r_{s,t}$ and $u_{s,t}$ must be jointly minimized in the objective function to approximate (6c). The polygonal inner approximation of (2d), (3a) and (4e) is shown in Fig. 1 (b). The inner approximation is then described by,

$$A_m p + B_m q \leq \overline{S} \cos(\pi/L) \qquad \forall m \in [0, L] \quad (6g)$$

where $A_m = \cos(2m\pi/L)$ and $B_m = \sin(2m\pi/L)$.

2.5 Methodology

In order to estimate the flexible region where the assets connected to a DSO multiple simulations are carried out. Figure 2 shows how the simulations are performed to determine the flexible region of DSO n.

First, maximum and minimum values of active $F_p^{n,\max}$, $F_p^{n,\min}$ and reactive $F_q^{n,\max}$, $F_q^{n,\min}$ flexibility are computed using (7a) - (7d) for all $t \in \Omega_t$ and DSOs $p \in \Omega_p$.

$$\min - \sum_{t \in \Omega_t} F_{p,t}^n + \sum_{t \in \Omega_t} \sum_{s \in \Omega_s} (u_{s,t}^n + r_{s,t}^n) \qquad \forall n \in \Omega_n \quad (7a)$$

$$\min \sum_{t \in \Omega_t} F_{p,t}^n + \sum_{t \in \Omega_t} \sum_{s \in \Omega_s} (u_{s,t}^n + r_{s,t}^n) \qquad \forall n \in \Omega_n \quad (7b)$$

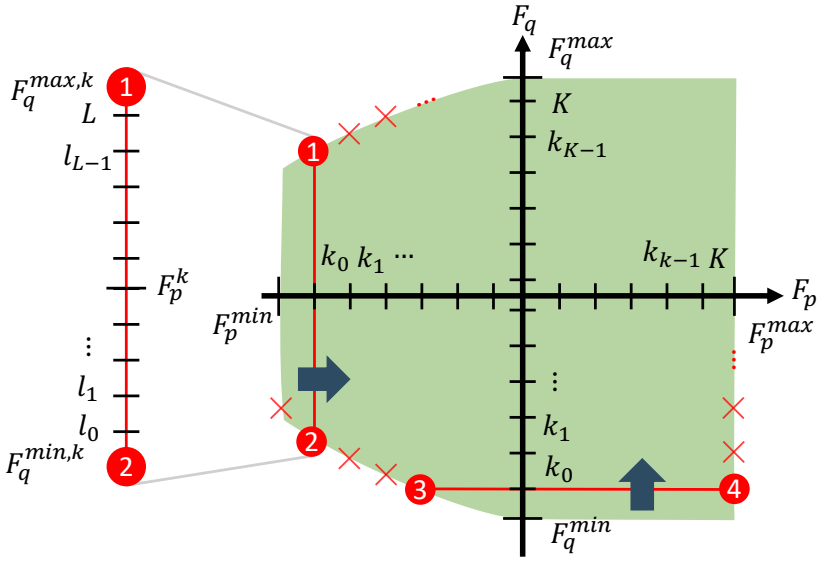

Figure 2: Methodology for the estimation of the feasible region in Multi-DSO LFMs.

$$\min -\sum_{t\in\Omega_t} F_{q,t}^n + \sum_{t\in\Omega_t}\sum_{s\in\Omega_s}(u_{s,t}^n + r_{s,t}^n) \qquad \forall n \in \Omega_n \quad (7c)$$

$$\min \sum_{t\in\Omega_t} F_{q,t}^n + \sum_{t\in\Omega_t}\sum_{s\in\Omega_s}(u_{s,t}^n + r_{s,t}^n) \qquad \forall n \in \Omega_n \quad (7d)$$

$$\min \sum_{t\in\Omega_t}\sum_{s\in\Omega_s}(u_{s,t}^n + r_{s,t}^n) \qquad \forall n \in \Omega_n \quad (7e)$$

After that, those dimensions are discretized K times as Fig. 2 shows. Points 1 and 2 are computed using objectives (7c) and (7d), respectively while fixing active flexibility using (7f). Points 3 and 4 are calculated using (7a) and (7b), respectively while fixing reactive flexibility using (7g). Additionally, the costs associated to each point of the flexible region are obtained using (5a).

$$F_{p,t}^n = F_{p,t}^{n,\min} + k(F_{p,t}^{n,\max} - F_{p,t}^{n,\min})/K \qquad \forall t \in \Omega_t \quad (7f)$$

$$F_{q,t}^n = F_{q,t}^{n,\min} + k(F_{q,t}^{n,\max} - F_{q,t}^{n,\min})/K \qquad \forall t \in \Omega_t \quad (7g)$$

Then, reactive dimension is discretized L times between points 1 and 2, as Fig. 2 shows. In these simulations, both the reactive and active flexibility are fixed, and the costs are the only output of the optimization problem. The methodology for estimating the Flexibility Region in Inter-DSO LFM is summarised in algorithm 1.

3 Case Study

Figure 3 lays out a case study based on the IEEE-34 test network. Without loss of generality, LFM is solved for periods of $\Delta t = 15$ minutes. Data used in this case study is available in [20]. Total static load of the case study is 611.84

Algorithm 1 Estimating Inter-DSO Flexibility Region

for $n \in \Omega_n$ **do**
  $F_{p,t}^{n,\max} \leftarrow \arg\min\{(7a) \text{ s.t. } (1)-(4)\}$
  $F_{p,t}^{n,\min} \leftarrow \arg\min\{(7b) \text{ s.t. } (1)-(4)\}$
  $F_{q,t}^{n,\max} \leftarrow \arg\min\{(7c) \text{ s.t. } (1)-(4)\}$
  $F_{q,t}^{n,\min} \leftarrow \arg\min\{(7d) \text{ s.t. } (1)-(4)\}$
  for $k = 1, 2, \ldots, K$ **do** ▷ Parallelized Loop
    $C_t^{n,k}, F_{p,t}^{n,\max,k} \leftarrow \arg\min\{(7a) \text{ s.t. } (1)-(4), (7g)\}$,
    $C_t^{n,k}, F_{p,t}^{n,\min,k} \leftarrow \arg\min\{(7b) \text{ s.t. } (1)-(4), (7g)\}$,
    $C_t^{n,k}, F_{q,t}^{n,\max,k} \leftarrow \arg\min\{(7c) \text{ s.t. } (1)-(4), (7f)\}$,
    $C_t^{n,k}, F_{q,t}^{n,\min,k} \leftarrow \arg\min\{(7d) \text{ s.t. } (1)-(4), (7f)\}$
    for $l = 1, 2, \ldots, L$ **do** ▷ Parallelized Loop
      $C_t^{k,l} \leftarrow \arg\min\{(7e) \text{ s.t. } (1)-(4), (7f), (7g)\}$
    end for
  end for
end for

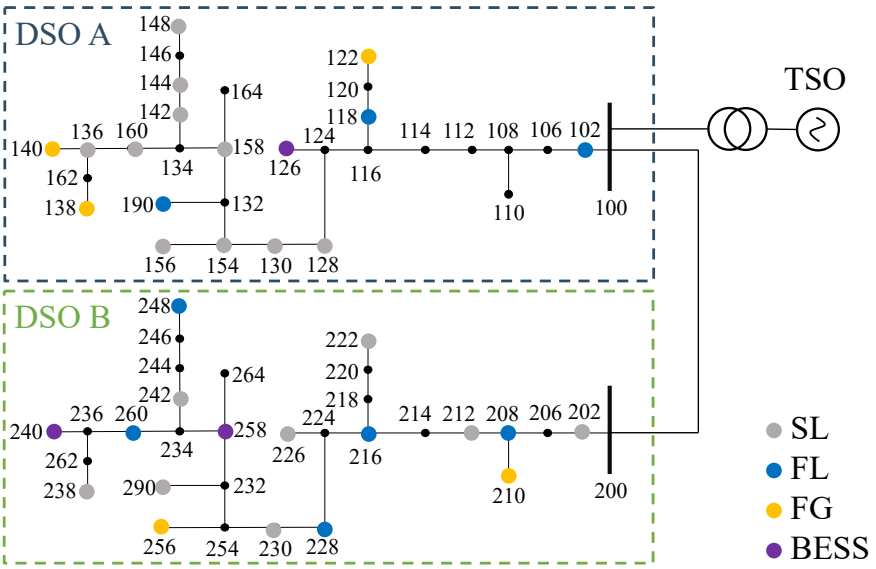

Figure 3: Case study based on two IEEE 34 bus networks representing the DSOs. Grey, blue, orange and purple dots represent Static Loads (SLs), FLs, FGs and BESSs, respectively.

kVA with 18 SLs, 8 FLs, 5 FGs and 3 BESSs distributed among two DSOs. The interface with the TSO is modelled using a generator connected to node 100. Flexible region is computed considering two situations; the first one where the TSO is in green state and can modify the power flow through the interface and, the second, where the interface is congested, and the flexibility should be exclusively exchanged among DSOs. Simulations were performed using GAMS 24.2.2 and CPLEX 12.6.3. on a cluster with 80 TB of RAM memory and 160 nodes of 2 x AMD EPYC 7H12 CPUs at 2.60 GHz, running Suse Leap 42 Linux

distribution.

3.1 Evolution of Flexibility Region with unrestricted interface

The evolution of the flexibility region and the associated costs of operation with the TSO providing as much flexibility as DSO needs is depicted in Fig. 4. Flexible region is computed using algorithm 1 for DSO A and B as Fig. 4a and 4b respectively show. In these figures, upward flexibility is represented in the positive semi-axis, while downward flexibility is depicted in the negative semi-axis. The penetration of solar renewable energy in FGs directly influences the final shape of the flexible region, increasing the size of the area at the central hours of the day.

In this situation, flexible region limits are showed in Table 1. DSO A obtains 191% and 141% more of upward active and reactive flexibility. In the downward direction, DSO A obtains 42% less of active flexibility, but 97% more of reactive flexibility. Although DSO A has wider upward flexibility, this came at the costs of having four time more expensive costs.

Table 1: Flexible region limits for DSO A and B with TSO in green state.

DSO A (TSO in green state)				
	Active Flex. (kW)		**Reactive Flex. (kVAr)**	
	Upward	Downward	Upward	Downward
Value	430.96	-79.52	741.61	-519.61
Time	13:00	20:00	13:00	00:15
Costs (€)	45.21	12.45	45.23	9.12
DSO B (TSO in green state)				
	Active Flex. (kW)		**Reactive Flex. (kVAr)**	
	Upward	Downward	Upward	Downward
Value	148.06	-137.46	307.6	-263.76
Time	13:00	20:00	11:45	00:00
Costs (€)	8.6	21.76	10.63	14.16

3.2 Estimation of Flexibility Region without TSO

The evolution of the flexibility region and its associated costs when the TSO cannot procure flexibility in the interconnection is depicted in Fig. 5. The overall volume of flexibility is reduced as (5b) is now enforced.

Flexible region limits are compared in Table 2. In this situation, DSO A can produce a 44% and 17% more of upward active and downward reactive flexibility, respectively. On the other hand, DSO B obtains a 30% and 15% more of downward active and upward reactive flexibility, respectively. Overall costs are reduces, however, DSO A still has nearly two times bigger costs than DSO B.

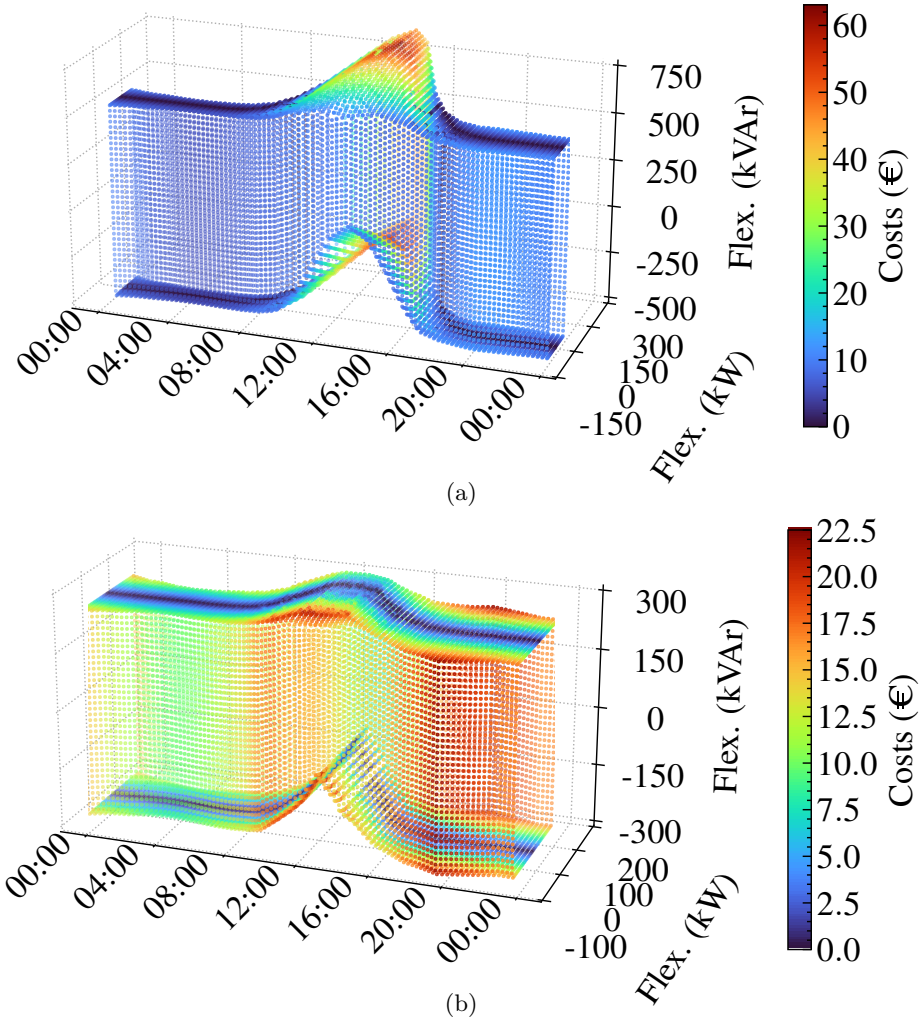

Figure 4: Flexible Region of DSO A (a) and DSO B (b) when the interface with TSO is not congested.

3.3 Evolution of the flexibility and its associated costs

The evolution of the area of the flexibility region over the day is represented in Fig. 6. Maximum flexibility is obtained when the TSO is in green state by DSO A. Flexible region area when the TSO is in emergency state is the same as depicted by Fig. 6.

Costs associated to the operation of the flexibility region are depicted in Fig. 7 for DSO A and in Fig. 8 for DSO B at different times of the day. Flexibility costs at nighttime are lower than costs at daylight, when they can reach 34 € for DSO A and 15 € for DSO B. The non-linearity of the problem appear in the non-uniform contour plots of the costs associated to each operation point.

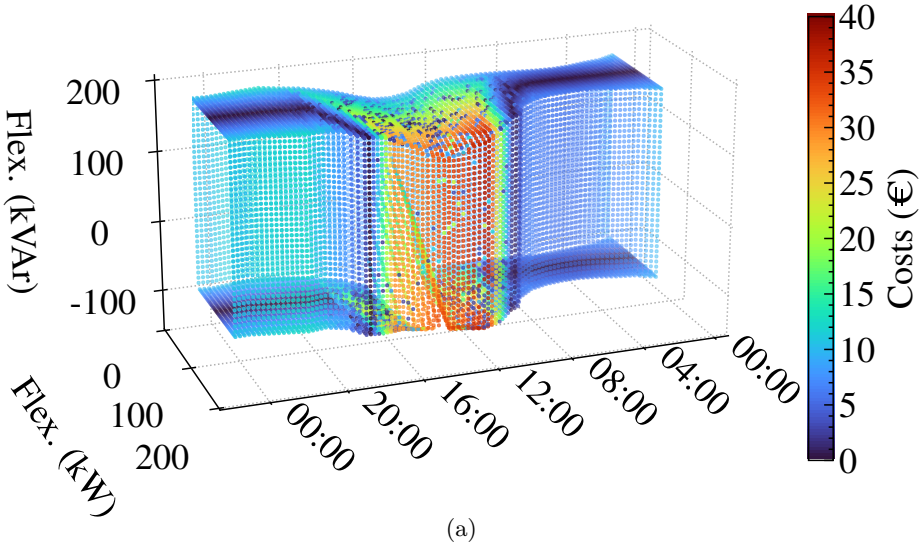

(a)

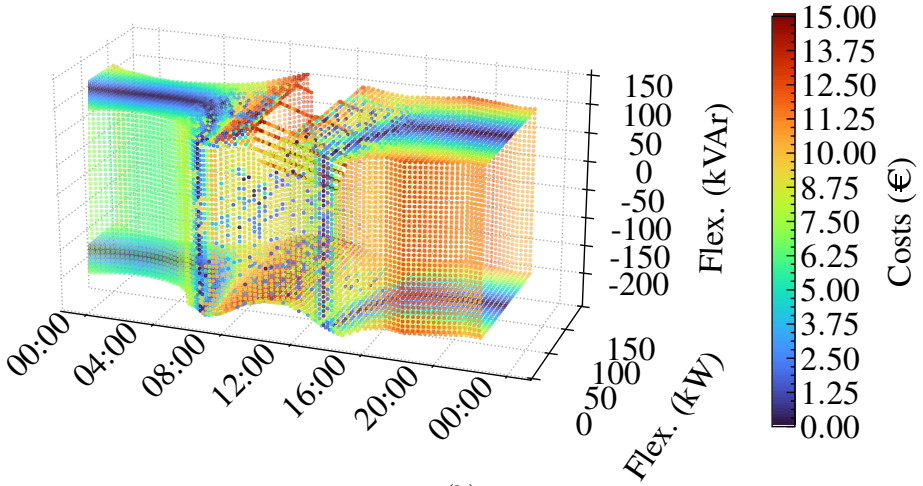

(b)

Figure 5: Flexible Region of DSO A (a) and DSO B (b) when the interface with TSO is congested.

4 Conclusions

This paper has presented a linear methodology to determine the flexibility region of DSOs participating in Inter-DSO LFMs. Non-linear behaviour of agents such as BESS are linearized using a variable change and McCormick envelopes, while quadratic constraints are linearized using a polygonal inner approximation. The proposed methodology is a valid tool for DSOs aiming to analyse their flexibility and the associated costs, no matter the situation of the upstream transmission network. Results based on the IEEE 34 bus network demonstrate the feasibility of the proposed approach to approximate the non-linearities of the model, while assessing the flexibility of DSOs, under high RDER penetration, when participating in LFMs.

Table 2: Flexible region limits for DSO A and B with TSO in emergency state.

DSO A (TSO in emergency state)				
	Active Flex. (kW)		**Reactive Flex. (kVAr)**	
	Upward	Downward	Upward	Downward
Value	114.37	-79.52	140.23	-164.05
Time	11:00	20:00	00:00	12:00
Costs (€)	3.09	12.45	9.66	26.48
DSO B (TSO in emergency state)				
	Active Flex. (kW)		**Reactive Flex. (kVAr)**	
	Upward	Downward	Upward	Downward
Value	79.52	-114.37	164.05	-140.23
Time	20:00	11:00	12:00	00:00
Costs (€)	12.45	6.08	13.21	9.08

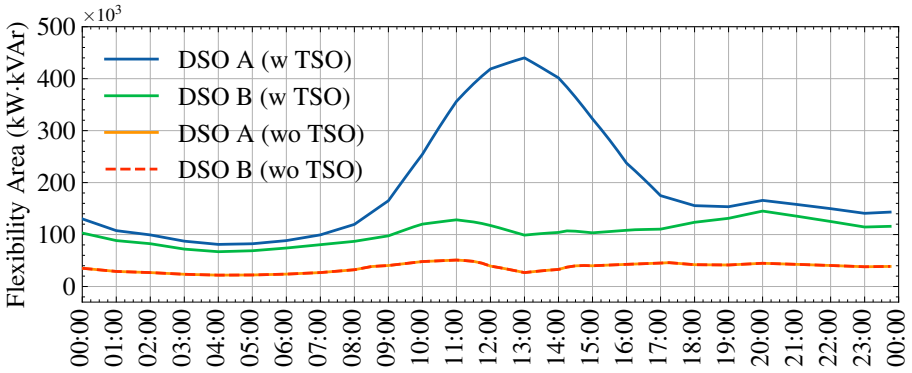

Figure 6: Evolution of the area of the flexible region for DSO A (blue) and DSO B (green) with TSO in green state, and for DSO A (orange) and DSO B (dashed red) with TSO in emergency state.

References

[1] A. Coelho, J. Iria, and F. Soares, "Network-secure bidding optimization of aggregators of multi-energy systems in electricity, gas, and carbon markets," *Appl. Energy*, vol. 301, no. July, 2021.

[2] M. I. Alizadeh, M. Usman, F. Capitanescu, and A. G. Madureira, "A Novel TSO-DSO Ancillary Service Procurement Coordination Approach for Congestion Management," in *2022 IEEE Power Energy Soc. Gen. Meet.* IEEE, jul 2022, pp. 1–5.

[3] Á. Paredes and J. A. Aguado, "Coordinated trading of capacity and balancing products in multi-area local flexibility markets," in *2022 IEEE Electrical Power and Energy Conference (EPEC)*, 2022.

[4] S. Riaz and P. Mancarella, "On feasibility and flexibility operating regions of virtual power plants and TSO/DSO interfaces," *2019 IEEE Milan PowerTech, PowerTech 2019*, pp. 1–6, 2019.

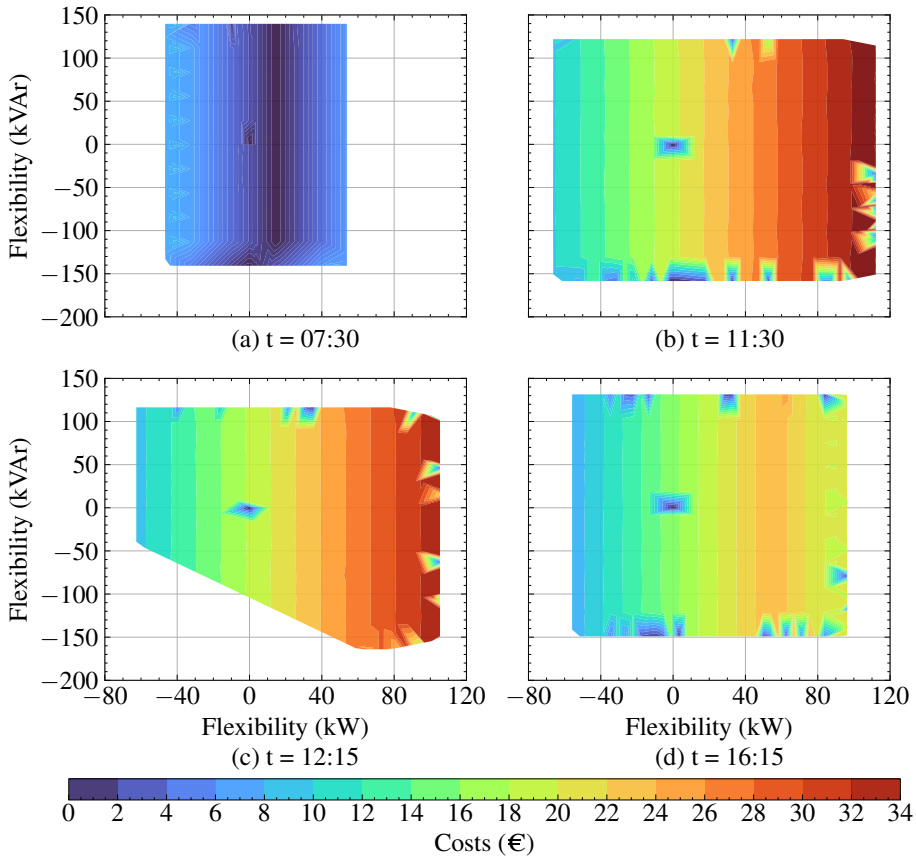

Figure 7: Contour plots of the costs associated to the flexible region of DSO A.

[5] L. Ageeva, M. Majidi, and D. Pozo, "Analysis of Feasibility Region of Active Distribution Networks," *Proc. 1st IEEE 2019 Int. Youth Conf. Radio Electron. Electr. Power Eng. REEPE 2019*, pp. 1–5, 2019.

[6] D. A. Contreras and K. Rudion, "Computing the feasible operating region of active distribution networks: Comparison and validation of random sampling and optimal power flow based methods," *IET Gener. Transm. Distrib.*, vol. 15, no. 10, pp. 1600–1612, 2021.

[7] J. Silva, J. Sumaili, R. J. Bessa, L. Seca, M. A. Matos, V. Miranda, M. Caujolle, B. Goncer, and M. Sebastian-Viana, "Estimating the Active and Reactive Power Flexibility Area at the TSO-DSO Interface," *IEEE Trans. Power Syst.*, vol. 33, no. 5, pp. 4741–4750, 2018.

[8] J. Silva, J. Sumaili, R. J. Bessa, L. Seca, M. Matos, and V. Miranda, "The challenges of estimating the impact of distributed energy resources flexibility on the TSO/DSO boundary node operating points," *Comput. Oper. Res.*, vol. 96, pp. 294–304, 2018.

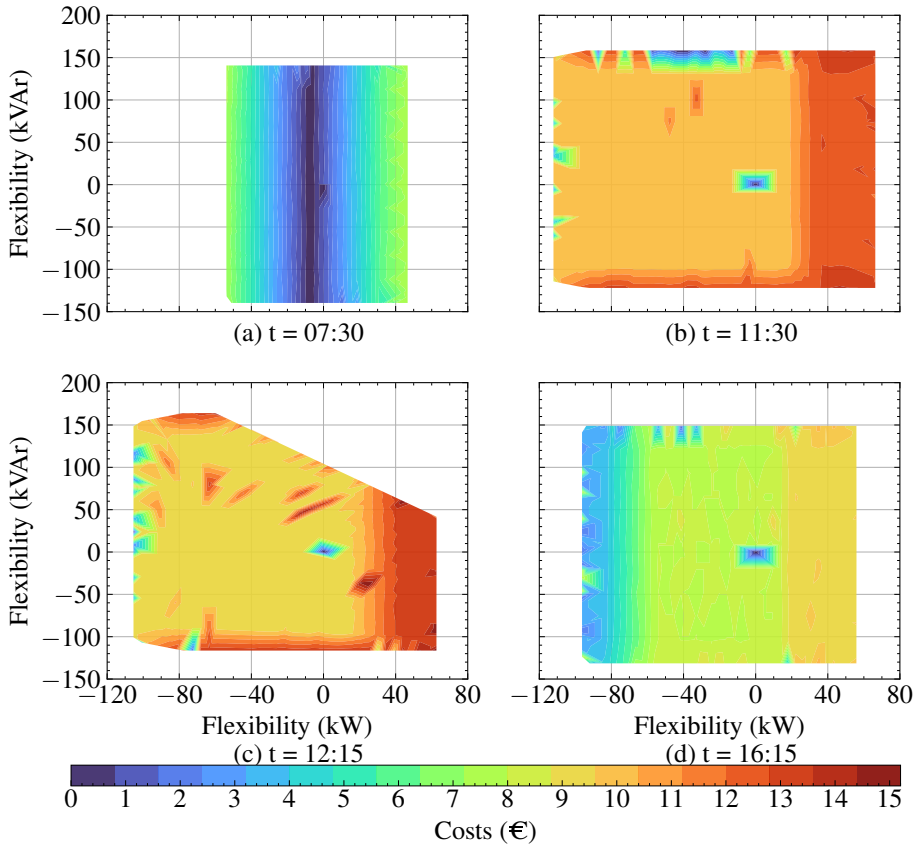

Figure 8: Contour plots of the costs associated to the flexible region of DSO B.

[9] N. Savvopoulos and N. Hatziargyriou, "Estimating Operational Flexibility from Active Distribution Grids," *Int. Conf. Eur. Energy Mark. EEM*, vol. 2020-Septe, 2020.

[10] L. Lopez, A. Gonzalez-Castellanos, D. Pozo, M. Roozbehani, and M. Dahleh, "QuickFlex: a Fast Algorithm for Flexible Region Construction for the TSO-DSO Coordination," in *2021 Int. Conf. Smart Energy Syst. Technol.* IEEE, sep 2021, pp. 1–6.

[11] F. Capitanescu, "TSO–DSO interaction: Active distribution network power chart for TSO ancillary services provision," *Electr. Power Syst. Res.*, vol. 163, no. March, pp. 226–230, 2018.

[12] L. Ageeva, M. Majidi, and D. Pozo, "Coordination between TSOs and DSOs: Flexibility Domain Identification," in *12th Mediterr. Conf. Power Gener. Transm. Distrib. Energy Convers. (MEDPOWER 2020)*. Institution of Engineering and Technology, 2021, pp. 429–434.

[13] S. Riaz and P. Mancarella, "Modelling and Characterisation of Flexibility from Distributed Energy Resources," *IEEE Trans. Power Syst.*, vol. 37, no. 1, pp. 38–50, 2022.

[14] M. Kalantar-Neyestanaki, F. Sossan, M. Bozorg, and R. Cherkaoui, "Characterizing the Reserve Provision Capability Area of Active Distribution Networks: A Linear Robust Optimization Method," *IEEE Trans. Smart Grid*, vol. 11, no. 3, pp. 2464–2475, 2020.

[15] S. Wang and W. Wu, "Aggregate Flexibility of Virtual Power Plants with Temporal Coupling Constraints," *IEEE Trans. Smart Grid*, vol. 12, no. 6, pp. 5043–5051, 2021.

[16] M. Alramlawi, A. Gabash, E. Mohagheghi, and P. Li, "Optimal Operation of PV-Battery-Diesel MicroGrid for Industrial Loads under Grid Blackouts," *Proc. - 2018 IEEE Int. Conf. Environ. Electr. Eng. 2018 IEEE Ind. Commer. Power Syst. Eur. EEEIC/I CPS Eur. 2018*, 2018.

[17] J. Yang, N. Zhang, C. Kang, and Q. Xia, "A State-Independent Linear Power Flow Model with Accurate Estimation of Voltage Magnitude," *IEEE Trans. Power Syst.*, vol. 32, no. 5, pp. 3607–3617, 2017.

[18] G. P. McCormick, "Computability of global solutions to factorable nonconvex programs: Part i —convex underestimating problems," *Mathematical Programming*, vol. 10, no. 1, pp. 147–175, 1976.

[19] K. Steriotis, K. Sepetanc, K. Smpoukis, N. Efthymiopoulos, P. Makris, E. Varvarigos, and H. Pandzic, "Stacked Revenues Maximization of Distributed Battery Storage Units Via Emerging Flexibility Markets," *IEEE Trans. Sustain. Energy*, vol. 13, no. 1, pp. 464–478, jan 2022.

[20] Ángel Paredes and José A. Aguado, "Local flexibility market dataset," 2022. [Online]. Available: https://doi.org/10.17632/6HT44TMVTF.1